Stabilizing the Garnet Solid-Electrolyte / Polysulfide Interface in Li-S Batteries

Kun (Kelvin) Fu,[1,2,(a)] Yunhui Gong,[1,2,(a)] Shaomao Xu,[1,2,(a)] Yizhou Zhu,[2] Yiju Li,[2] Jiaqi Dai,[2] Chengwei Wang,[1,2] Boyang Liu,[2] Glenn Pastel,[2] Hua Xie,[2] Yonggang Yao,[2] Yifei Mo,[1,2] Eric Wachsman,[1,2,*] Liangbing Hu[1,2,*]

[1]University of Maryland Energy Research Center, University of Maryland, College Park, Maryland, 20742

[2]Department of Materials Science and Engineering, University of Maryland, College Park, Maryland, 20742

[(a)] Equally contributed

* Corresponding author: binghu@umd.edu; ewach@umd.edu

Abstract

Garnet type solid electrolyte, having high ionic conductivity and large electrochemical stability window, can be a promising dense ceramic membrane in Li-metal batteries. Among solid electrolytes, garnet solid electrolytes are so far the only material that is chemically compatible with Li metal. The integration of garnet solid electrolyte is paramount to addressing the challenges of chemical and physical short circuits in Li-S batteries, such as Li dendrite penetration and polysulfide shuttling. However, the stability of garnet solid electrolyte with sulfur-based cathode materials remain unknown. A great understanding of garnet solid electrolyte and its electro/chemical compatibility with sulfur cathode materials is therefore urgently needed. In this work, we investigated the interface chemical stability of garnet-type solid electrolyte with polysulfides. Experimental and computational results show that an interphase layer may form once Li_2S and Li_2SO_4 are formed, which can protect the garnet electrolyte from further reaction. This discovery illustrates that garnet-type solid-state electrolytes are electro/chemically stable against sulfur/intermediate species and LiTFSI liquid electrolyte. We also demonstrate a full cell using garnet solid electrolyte to evaluate its electrochemical performance, showing a high rate capability (1 mA/cm^2) and long-term cycling stability with good capacity retention.

Chemical and physical short circuits are the main challenges faced by lithium batteries which compromise battery performance and safety.[1,2] At the cathode, solvation of active cathode materials and shuttling of unwanted chemical species in the liquid electrolyte result in "chemical short circuits", which deteriorate the Li metal electrode and limit the deployment of new cathode materials, such as high voltage cathodes, sulfur, and air/O_2. In Li-S batteries, the repeated shuttling of polysulfides between electrodes constantly corrodes the Li metal anode and the loss of active material will result in low coulombic efficiency.[3] At the anode, Li dendrite penetration through the separator causes internal electronic, or "physical", short circuits. Several strategies have been reported to prevent chemical and physical short circuits by using a cathode host, small sulfur molecules, modified separators, or electrolyte additives to alleviate sulfur materials diffusion and shuttling, and finding ways to delay, confine, or block Li dendrites to extend the cycling lifetime and avoid thermal runaway in lithium-metal batteries.[4–12]

The integration of solid-state electrolytes with liquid electrolytes is a promising way to simultaneously address the challenges associated with chemical and physical short circuits.[13] In the hybrid design, the liquid electrolyte maintains fast ion transport kinetics while the solid-state electrolyte serves as a rigid barrier to separate electrodes and block the transport of unwanted chemical species and Li dendrite penetration and extensive studies have been reported to use LISICON and NASICON type solid electrolyte in Li metal batteries.[14–19] However, some solid electrolytes have low ionic conductivity and some solid electrolyte materials may have side reactions with Li and decomposition will occur at interface, which cannot be used for Li metal batteries.

Among different types of solid-state electrolytes, garnet-type $Li_7La_3Zr_2O_{12}$ (LLZO) has been proven to be the most promising Li ion solid-state electrolyte for its high ionic conductivity (10^{-4}

S/cm), superior interfacial stability with Li metal, and large electrochemical window, which is the ideal solid electrolyte for Li-metal batteries.[20–26] Extensive studies of garnet solid electrolytes and their application in batteries have been reported. Our recent work have successfully addressed the solid-solid interface of garnet electrolyte and metallic Li and confirmed the long-term cycling stability of garnet solid electrolyte in symmetric Li/solid electrolyte/Li cells.[27–29] We applied atomic layer deposition (ALD) to decrease the interfacial resistance of garnet and Li metal from thousands of ohm·cm^2 to a few ohm·cm^2.[28] However, the electro/chemical stability between garnet solid electrolyte and polysulfides, which are the main products of sulfur cathode, remains unknown. In this work, we are focusing on the garnet solid electrolyte and sulfur cathodes to investigate the interface stability of garnet solid electrolyte with polysulfides (Li_2S_8) and Li_2S, which are the main products of reduced sulfur species, and demonstrate a full cell using garnet solid electrolyte in Li-S batteries (Figure 1). We have carried out a series of characterizations including XPS, XRD, Raman, and TEM to study the chemical stability of garnet solid electrolyte with polysulfides, and used first principle calculations to study the thermodynamic reaction energy of garnet solid electrolyte with Li_2S and Li_2S_8. Based on this study, a full Li-S cell using garnet solid electrolyte was demonstrated, showing high rate performance (1 mA/cm^2) and superior cycling stability with good capacity retention.

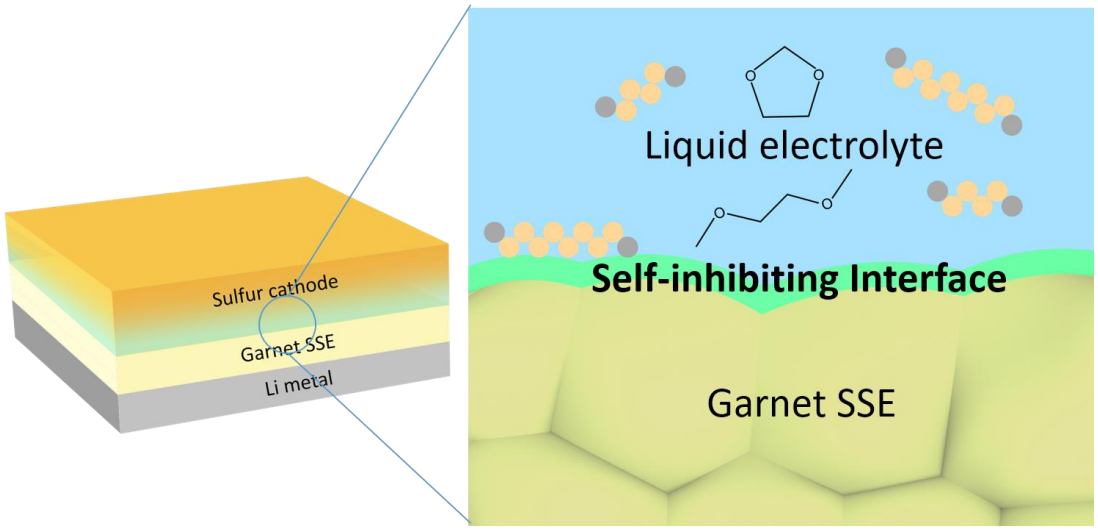

Figure 1. Schematic of solid-liquid electrolyte interface in hybrid Li-S battery. Garnet solid electrolyte has interface with liquid electrolyte (LiTFSI in DME/DOL) and soluble polysulfides (e.g. Li_2S_8, Li_2S_4.). The self-inhibiting interface helps to protect the garnet solid electrolyte from polysulfides and liquid electrolyte environment.

To determine the compatibility of garnet solid electrolyte in a liquid Li-S system, experiments were carried out by immersing a dense garnet disk (~200 μm), as a model system, in lithium polysulfide solution (Li_2S_8 dissolved in DME/DOL) and liquid electrolyte (LiTFSI in DME/DOL). The surface of the garnet pellet was scrubbed with sand paper to remove Li_2CO_3, followed by immersing in liquid electrolyte or lithium polysulfide solution for one week. The garnet was then rinsed by DME/DOL solvent and dried before characterization. To prevent samples contacting with oxygen and moisture, we transfer the samples to the chamber in an argon-filled bag. After immersing in Li_2S_8/DME/DOL, significant SO_4^{-2} and S_2^{-2} peaks were detected on the garnet surface by X-ray photoelectron spectroscopy analysis (XPS) (Figure 2a). These peaks are corresponding to Li_2SO_4 and Li_2S. After 30 minutes of Ar ion sputtering to clean the surface, a S^{-2} signal was detected with a sharp peak and high intensity (Figure 2b). The $S_2^{-2}$and S^{-2} peaks

most likely originate from Li_2S_2 and Li_2S, which are decomposition products of the lithium polysulfide Li_2S_8. The Zr 3d spectra of garnet with and without ion sputtering in Figure 2c shows that before sputtering, there is no Zr 3d peak detected on the garnet surface. However, after sputtering, a Zr 3d peak was detected, which indicates the formation of a solid interphase with finite thickness on the garnet surface.

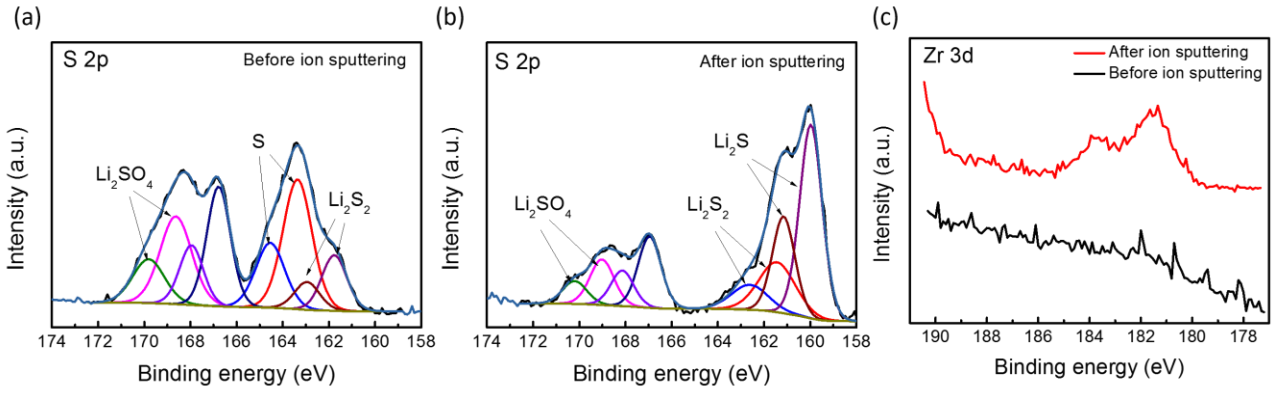

Figure 2. (a-b) S 2p XPS spectra of dense garnet pellet before and after Ar sputtering on surface. Before XPS analysis, the dense garnet pellet was fully immersed in polysulfides solution (Li_2S_8 in DME/DOL) for 1 week. (c) Zr 3d XPS spectra of dense garnet pellet before and after Ar sputtering on surface.

To characterize the phase structure, garnet powders were used to soak into liquids: LiTFSI/DME/DOL and Li_2S_8/DME/DOL, respectively. Garnet powders have higher surface area compared to garnet disk and thus have more exposure to liquids. The X-ray diffraction patterns (XRD) in Figure 3a indicate that garnet powders remain in the cubic phase. Although the XPS results indicate that liquid electrolyte and garnet solid electrolyte were decomposed to a certain extent in polysulfide solution, the stable cubic phase and electrochemical performance in Li-S full cells demonstrate sufficient practical stability for application. Raman spectra of garnet powder

treated under the same conditions confirm that the garnet cubic structure remained stable (Figure 3b). To further understand the morphology change, we conducted high-resolution transmission electron microscopy (TEM) to the pristine garnet powders and electrolyte soaked garnet powders. For the pristine garnet powder, a highly crystalized structure can be observed on the surface (Figure S1). For the electrolyte soaked garnet power, an amorphous layer with a thickness of ~5 nm can be observed on the surface, which is possibly due to decomposition of the garnet at the electrolyte interphase (Figure 3c). To further examine the chemical stability with sulfur, we mixed garnet nanopowders with elemental sulfur in a mass ratio of 1:5 and heated the mixture at 160ºC for 24 hours to characterize garnet powders phase structure. The garnet powder/sulfur mixture was then washed with carbon disulfide (CS_2) to cleanse them of sulfur before characterizing the structure by XRD. The XRD pattern in Figure 3d confirms the same cubic structure as the standard garnet LLZO XRD pattern, indicating the good chemical stability with sulfur.

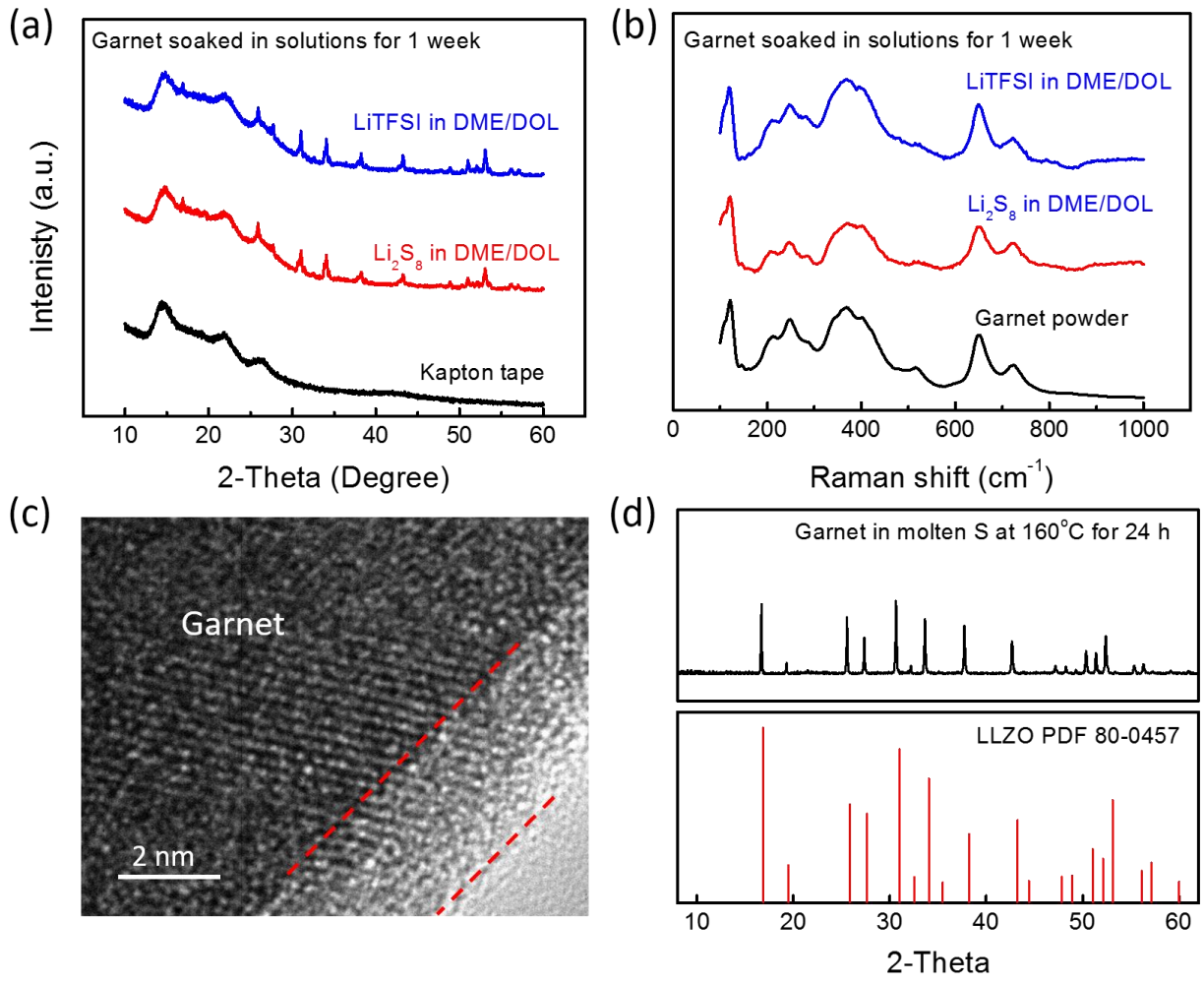

Figure 3. (a-b) XRD patterns and Raman spectra of garnet powders after being soaked in liquid electrolyte (LiTFSI in DME/DOL) and polysulfides solution for one week. The samples were sealed in a Kapton bag to avoid oxygen and moisture contamination. (c) TEM image of garnet nanopowders after being soaked in polysulfides solution for 1 week. (d) XRD pattern of garnet powders after being soaked in molten sulfur at 160ºC for one week.

In addition, first principle calculations were carried out to investigate the chemical stability of garnet electrolytes with reduced sulfur species. The same approach as in our previous study was used to identify the most thermodynamically favorable phase equilibria as a potential interphase

layer formed between LLZO garnet and lithium polysulfides.[26] We found that garnet has thermodynamically favorable reactions with polysulfide Li_2S_8, but is stable against Li_2S (Figure 4 and Table S1). The reaction products contain lithium sulfate and lithium sulfide, which are in good agreement with our XPS results. An interphase layer composed of Li_2S and Li_2SO_4 can provide passivation and stop interfacial reactions from growing into the bulk garnet. Therefore, both computational and experimental results indicate a self-inhibiting interphase layer formation may occur at the interface once Li_2S is formed to protect garnet from further reactions. Our conclusions are consistent with a recent study that reports a solid-liquid electrolyte interphase (SLEI) due to decomposition of both the solid and organic electrolytes.[1]

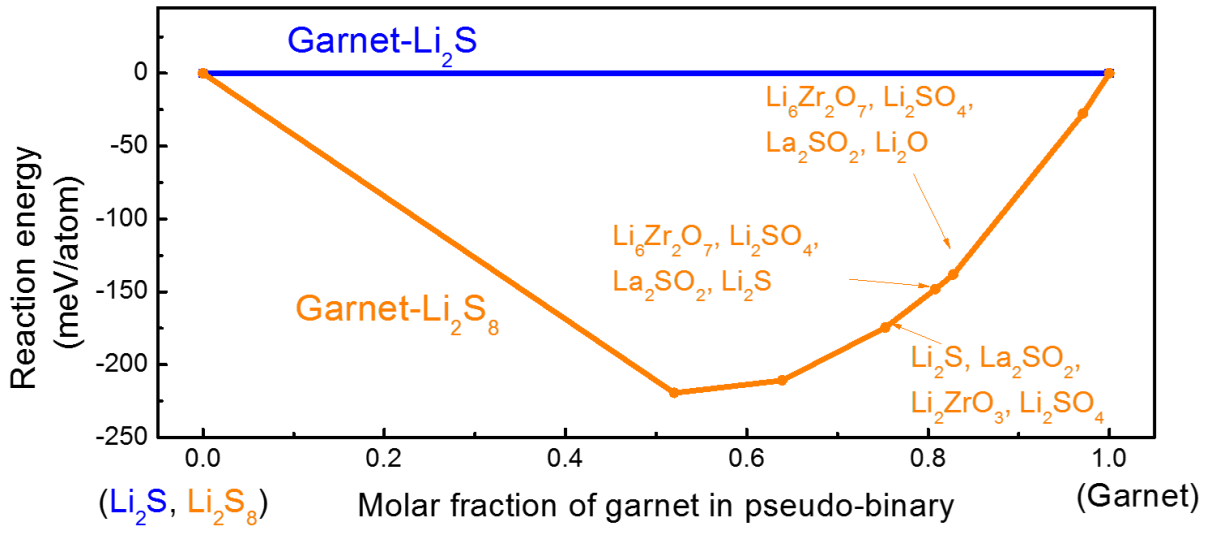

Figure 4. Calculated reaction energy of garnet LLZO with Li_2S and Li_2S_8. Garnet has thermodynamically favorable reactions with polysulfide Li_2S_8, but is stable against Li_2S. An interphase layer composed of Li_2S and Li_2SO_4 can provide passivation and stop interfacial reactions from growing into the bulk garnet.

Electrochemical performance of Li-S batteries using the solid-state garnet hybrid electrolyte is shown in Figure 5. A schematic comparing the Li-S battery with conventional and solid-state electrolyte membrane is shown in Figure 5a. The soluble polysulfides can diffuse through porous polymer separator and migrate to the Li metal anode, but cannot penetrate through the dense ceramic ion conductor, thus avoiding polysulfides shuttle effect, side reactions on Li, and Li metal corrosion. Polysulfide shuttling behavior occurs while charging as shown in Figure 5b. The extended charge voltage plateau is typical of polysulfide shuttling, causing longer charging times before achieving the upper cut-off voltage. The fast capacity decay and low coulombic efficiency in conventional Li-S batteries (Supplementary Figure S2) ask for the urgent need to use hybrid solid-state configuration. The hybrid cell was then assembled into a 2032 coin cell with a highly conductive carbon sponge. The carbon sponge acted as the force absorber and prevented the garnet ceramic disk from being damaged. The edge of the cell was sealed with epoxy resin. In hybrid cell, there is no extended charging plateau, and the capacity value is reasonable with a coulombic efficiency close to 100%. The hybrid electrolyte delivered stable cycling performance without polysulfide shuttling (Supplementary Figure S3).

Figure 5c shows the discharge and charge curves of a hybrid cell at different current densities. The hybrid cell was made by using a dense garnet (<50 μm) and a slurry-casted sulfur cathode and packaged in coin cells. The coin cells were sealed by using epoxy resin. The sulfur mass loading was ~1.2 mg/cm^2. Regular liquid electrolyte (LiTFSI in DME/DOL) was used as a liquid electrolyte. Note that no $LiNO_3$ was added in the liquid electrolyte. At a current density of 200 mA/g, the sulfur cathode delivered a specific capacity of ~1000 mAh/g with a 100% coulombic efficiency. With a current density of 800 mA/g (corresponding to ~ 1mA/cm^2), the specific capacity was 550 mAh/g and the cell maintained a high coulombic efficiency close to 100%. The

rate performance is shown in Figure 5d. The hybrid cell showed good cycling stability at elevated current density and a good capacity retention at smaller currents.

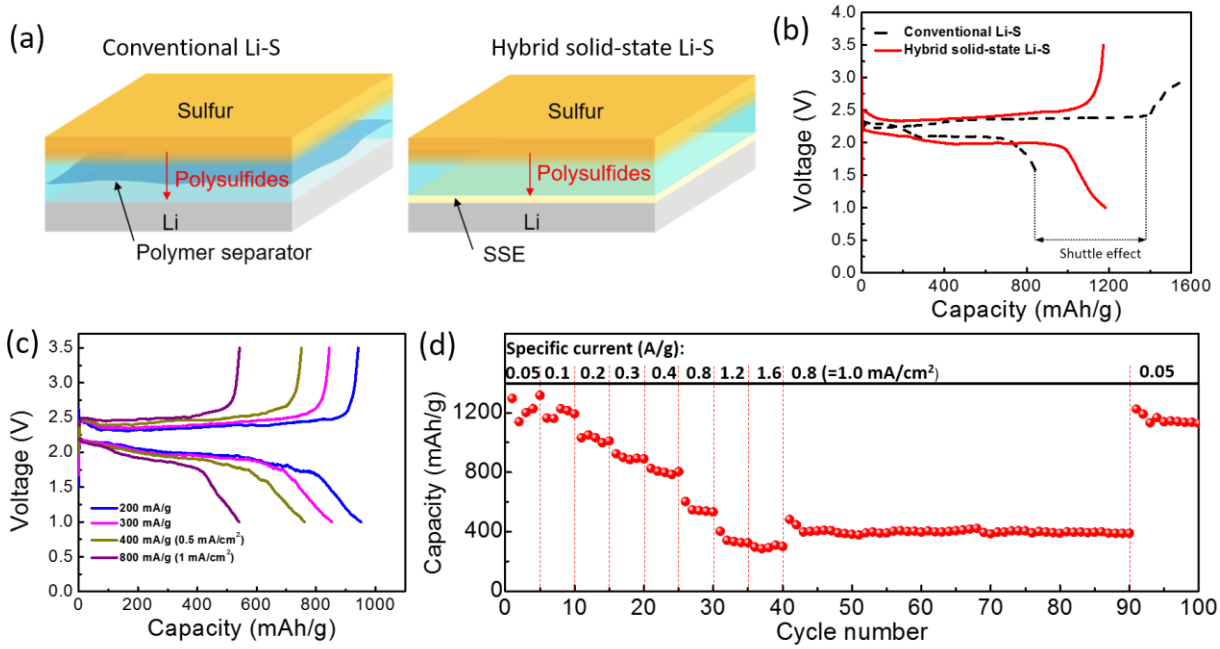

Figure 5. Electrochemical characterization of hybrid solid-state Li-S batteries. (a) Schematic of conventional Li-S and hybrid solid-state Li-S batteries. In conventional Li-S, polymeric porous membrane can neither block polysulfides nor prevent Li dendrite penetration. In hybrid solid-state Li-S batteries, the ceramic dense membrane cannot only physically block liquid electrolyte and polysulfides, but also suppress Li dendrite growth towards cathode. (b) Voltage profiles of conventional and hybrid Li-S cells. An extended plateau in charge plateau indicates the shuttle effect of polysulfides in conventional Li-S. No shuttle effect occurs in the hybrid Li-S cell. (c) Voltage profiles of hybrid Li-S cell at elevated current density. Dense garnet membrane and slurry-casted sulfur electrode with a mass loading of ~1.2 mg/cm^2 were assembled into the hybrid cell. (d) Rate performance of the hybrid Li-S cell.

In summary, we for the first time studied garnet-type solid electrolyte electro/chemical stability with sulfur cathode materials and demonstrated a Li-S battery using dense garnet solid ceramic membrane with high rate performance (1 mA/cm^2) and good capacity retention. Garnet solid electrolyte is the most promising solid electrolyte for use in Li-metal batteries, due to its stable interface with Li metal, high ionic conductivity, and large electrochemical window. Based on this work, garnet solid electrolyte exhibits a good stability with polysulfides by forming a self-inhibiting interlayer at the surface. Experimental results indicate that the garnet phase structure remained stable and an interphase layer with a thickness of ~5 nm was formed in the polysulfide environment, and computational study shows that this interface contains electron insulator Li_2S and Li_2SO_4, serving as a protective layer to prevent garnet solid electrolyte from further reactions. The Li-S battery based on garnet solid electrolyte exhibited a high coulombic efficiency of 100% and no polysulfide shuttling effect was observed in this Li-S system. This work shows the promising feasibility of using garnet type solid electrolyte with good electro/chemical stability in Li-S battery to address the polysulfides shuttling effect as well as Li dendrite short-circuiting.

Reference

(1) Busche, M. R.; Drossel, T.; Leichtweiss, T.; Weber, D. A.; Falk, M.; Schneider, M.; Reich, M.; Sommer, H.; Adelhelm, P.; Janek, J. Dynamic Formation of a Solid-Liquid Electrolyte Interphase and Its Consequences for Hybrid-Battery Concepts. *Nat. Chem.* **2016**, *8* (May), 426–434.

(2) Lin, D.; Liu, Y.; Cui, Y. Reviving the Lithium Metal Anode for High-Energy Batteries. *Nat. Nanotechnol.* **2017**, *12*, 194–206.

(3) Pang, Q.; Liang, X.; Kwok, C. Y.; Nazar, L. F. Advances in Lithium–sulfur Batteries Based on Multifunctional Cathodes and Electrolytes. *Nat. Energy* **2016**, *1* (9), 16132.

(4) Bai, S.; Liu, X.; Zhu, K.; Wu, S.; Zhou, H. Metal–organic Framework-Based Separator for Lithium–sulfur Batteries. *Nat. Energy* **2016**, *1* (7), 16094.

(5) Suo, L.; Hu, Y.-S.; Li, H.; Armand, M.; Chen, L. A New Class of Solvent-in-Salt Electrolyte for High-Energy Rechargeable Metallic Lithium Batteries. *Nat. Commun.* **2013**, *4*, 1481.

(6) Ji, X.; Lee, K. T.; Nazar, L. F. A Highly Ordered Nanostructured Carbon-Sulphur Cathode for Lithium-Sulphur Batteries. *Nat. Mater.* **2009**, *8* (6), 500–506.

(7) Lin, D.; Zhuo, D.; Liu, Y.; Cui, Y. All-Integrated Bifunctional Separator for Li Dendrite Detection via Novel Solution Synthesis of a Thermostable Polyimide Separator. *J. Am. Chem. Soc.* **2016**, *138* (34), 11044–11050.

(8) Liang, Z.; Lin, D.; Zhao, J.; Lu, Z.; Liu, Y.; Liu, C.; Lu, Y.; Wang, H.; Yan, K.; Tao, X.; Cui, Y. Composite Lithium Metal Anode by Melt Infusion of Lithium into a 3D Conducting Scaffold with Lithiophilic Coating. *Proc. Natl. Acad. Sci.* **2016**, *113* (11), 201518188.

(9) Tikekar, M. D.; Choudhury, S.; Tu, Z.; Archer, L. A. Design Principles for Electrolytes and Interfaces for Stable Lithium-Metal Batteries. *Nat. Energy* **2016**, *1* (9), 16114.

(10) Xin, S.; You, Y.; Wang, S.; Gao, H.; Yin, Y.; Guo, Y. Solid-State Lithium Metal Batteries Promoted by Nanotechnology: Progress and Prospects. *ACS Energy Lett.* **2017**, *2*, 1385–1394.

(11) Yang, C. P.; Yin, Y. X.; Guo, Y. G.; Wan, L. J. Electrochemical (De)lithiation of 1D Sulfur Chains in Li-S Batteries: A Model System Study. *J. Am. Chem. Soc.* **2015**, *137* (6), 2215–2218.

(12) Xin, S.; Gu, L.; Zhao, N.; Yin, Y.; Zhou, L.; Guo, Y.; Wan, L. Smaller Sulfur Molecules Promise Better Lithium − Sulfur Batteries. *J. Am. Chem. Soc.* **2012**, *134*, 18510–18513.

(13) Manthiram, A.; Yu, X.; Wang, S. Lithium Battery Chemistries Enabled by Solid-State Electrolytes. *Nat. Rev. Mater.* **2017**, *2* (3), 16103.

(14) Yu, X.; Bi, Z.; Zhao, F.; Manthiram, A. Polysulfide-Shuttle Control in Lithium-Sulfur Batteries with a Chemically/Electrochemically Compatible NaSICON-Type Solid Electrolyte. *Adv. Energy Mater.* **2016**.

(15) Yu, X.; Bi, Z.; Zhao, F.; Manthiram, A. Hybrid Lithium-Sulfur Batteries with a Solid Electrolyte Membrane and Lithium Polysulfide Catholyte. *ACS Appl. Mater. Interfaces* **2015**, *7*, 16625–16631.

(16) Wang, Q.; Jin, J.; Wu, X.; Ma, G.; Yang, J.; Wen, Z. A Shuttle Effect Free Lithium Sulfur Battery Based on a Hybrid Electrolyte. *Phys. Chem. Chem. Phys.* **2014**, *16*, 21225–21229.

(17) Wang, L.; Wang, Y.; Xia, Y. A High Performance Lithium-Ion Sulfur Battery Based on a Li2S Cathode Using a Dual-Phase Electrolyte. *Energy Environ. Sci.* **2015**, *8*, 1551–1558.

(18) Kitaura, H.; Zhou, H. All-Solid-State Lithium-Oxygen Battery with High Safety in Wide Ambient Temperature Range. *Sci. Rep.* **2015**, *5*, 13271.

(19) Yu, X.; Bi, Z.; Zhao, F.; Manthiram, A. Polysulfide-Shuttle Control in Lithium-Sulfur Batteries with a Chemically / Electrochemically Compatible NaSICON-Type Solid Electrolyte. *Adv. Energy Mater.* **2016**, 6, 1601392.

(20) Murugan, R.; Thangadurai, V.; Weppner, W. Schnelle Lithiumionenleitung in Granatartigem Li7La3Zr2O12. *Angew. Chemie* **2007**, *119*, 7925–7928.

(21) Fu, K. (Kelvin); Gong, Y.; Dai, J.; Gong, A.; Han, X.; Yao, Y.; Wang, C.; Wang, Y.; Chen, Y.; Yan, C.; Li, Y.; Wachsman, E. D.; Hu, L. Flexible, Solid-State, Ion-Conducting Membrane with 3D Garnet Nanofiber Networks for Lithium Batteries. *Proc. Natl. Acad. Sci.* **2016**, *113*, 7094–7099.

(22) Van den Broek, J.; Afyon, S.; Rupp, J. L. M. Interface-Engineered All-Solid-State Li-Ion Batteries Based on Garnet-Type Fast Li+ Conductors. *Adv. Energy Mater.* **2016**, *6*, 1600736.

(23) Thangadurai, V.; Narayanan, S.; Pinzaru, D. Garnet-Type Solid-State Fast Li Ion Conductors for Li Batteries: Critical Review. *Chem. Soc. Rev.* **2014**, *43*, 4714–4727.

(24) Thompson, T.; Sharafi, A.; Johannes, M. D.; Huq, A.; Allen, J. L.; Wolfenstine, J.;

Sakamoto, J. A Tale of Two Sites: On Defining the Carrier Concentration in Garnet-Based Ionic Conductors for Advanced Li Batteries. *Adv. Energy Mater.* **2015**, *5*, 1–9.

(25) Zhu, Y.; He, X.; Mo, Y. Origin of Outstanding Stability in the Lithium Solid Electrolyte Materials: Insights from Thermodynamic Analyses Based on First-Principles Calculations. *ACS Appl. Mater. Interfaces* **2015**, *7*, 23685–23693.

(26) Zhu, Y.; He, X.; Mo, Y. First Principles Study on Electrochemical and Chemical Stability of the Solid Electrolyte-Electrode Interfaces in All-Solid-State Li-Ion Batteries. *J. Mater. Chem. A* **2015**, *4*, 3253–3266.

(27) Luo, W.; Gong, Y.; Zhu, Y.; Fu, K. K.; Dai, J.; Lacey, S. D.; Wang, C.; Liu, B.; Han, X.; Mo, Y.; Wachsman, E. D.; Hu, L. Transition from Superlithiophobicity to Superlithiophilicity of Garnet Solid-State Electrolyte. *J. Am. Chem. Soc.* **2016**, *138*, 12258–12262.

(28) Han, X.; Gong, Y.; Fu, K. (Kelvin); He, X.; Hitz, G. T.; Dai, J.; Pearse, A.; Liu, B.; Wang, H.; Rubloff, G.; Mo, Y.; Thangadurai, V.; Wachsman, E. D.; Hu, L. Negating Interfacial Impedance in Garnet-Based Solid-State Li Metal Batteries. *Nat. Mater.* **2016**, *1* (December).

(29) Wang, C.; Gong, Y.; Liu, B.; Fu, K.; Yao, Y.; Hitz, E.; Li, Y.; Dai, J.; Xu, S.; Luo, W.; Wachsman, E. D.; Hu, L. Conformal, Nanoscale ZnO Surface Modification of Garnet-Based Solid-State Electrolyte for Lithium Metal Anodes. *Nano Lett.* **2016**, acs.nanolett.6b04695.

(30) Jain, A.; Ong, S. P.; Hautier, G.; Chen, W.; Richards, W. D.; Dacek, S.; Cholia, S.; Gunter, D.; Skinner, D.; Ceder, G.; Persson, K. A. Commentary: The Materials Project: A Materials Genome Approach to Accelerating Materials Innovation. *APL Mater.* **2013**, *1*, 11002.

(31) Ong, S. P.; Wang, L.; Kang, B.; Ceder, G. Li−Fe−P−O 2 Phase Diagram from First Principles Calculations. *Chem. Mater.* **2008**, *20*, 1798–1807.

Competing Interests

The authors declare no competing financial interests.

Acknowledgement

This work was supported by the US Department of Energy EERE (Contract No. DE-EE0006860) and NASA Advanced Energy Storage System Project, within the Game Changing Development Program of the Space Technology Mission Directorate. We also acknowledge the support of the Maryland NanoCenter and its AIMLab.

Stabilizing the Garnet Solid-Electrolyte / Polysulfide Interface in Li-S Batteries

Kun (Kelvin) Fu,[1,2,(a)] Yunhui Gong,[1,2,(a)] Shaomao Xu,[1,2,(a)] Yizhou Zhu,[2] Yiju Li,[2] Jiaqi Dai,[2] Chengwei Wang,[1,2] Boyang Liu,[2] Glenn Pastel,[2] Hua Xie,[2] Yonggang Yao,[2] Yifei Mo,[1,2] Eric Wachsman,[1,2,*] Liangbing Hu[1,2,*]

[1]University of Maryland Energy Research Center, University of Maryland, College Park, Maryland, 20742

[2]Department of Materials Science and Engineering, University of Maryland, College Park, Maryland, 20742

[(a)] Equally contributed

* Corresponding author: binghu@umd.edu; ewach@umd.edu

Experimental

Garnet solid-state electrolyte preparation. The LLCZN powder was synthesized *via* a modified sol-gel method. The starting materials were $LiNO_3$ (99%, Alfa Aesar), $La(NO_3)_3$ (99.9%, Alfa Aesar), $Ca(NO_3)_2$ (99.9%, Sigma Aldrich), $ZrO(NO_3)_2$ (99.9%, Alfa Asear) and $NbCl_5$ (99.99%, Alfa Aesar). Stoichiometric amounts of these chemicals were dissolved in de-ionized water and 10% excess $LiNO_3$ was added to compensate for lithium volatilization during the high temperature pellet preparation. Citric acid and ethylene glycol (1:1 mole ratio) were added to the solution. The solution was evaporated at 120ºC for 12h to produce the precursor gel and then calcined to 400ºC and 800ºC for 5 hours to synthesize the garnet powder. The garnet powders were uniaxially pressed into pellets and sintered at 1050ºC for 12 hours covered by the same type of powder for conductivity and stability experiments.

Material characterization. Phase analysis was performed by powder X-ray diffraction (XRD) on a D8 Advanced with LynxEye and SolX (Bruker AXS, WI, USA) using a Cu Kα radiation source operated at 40 kV and 40 mA. The morphology of the samples was examined by a field emission scanning electron microscope (FE-SEM, JEOL 2100F). Raman characterization was done with a Horiba Jobin-Yvon with the laser wavelength at 532 nm and the integration time of 4 seconds repeated for 4 times.

First Principles Computation. We considered the interface as a pseudo-binary of Li_2S/Li_2S_8 and garnet using the same approach as defined in previous work.[26] The phase diagrams were constructed to identify possible thermodynamically favorable reactions. The energies for the materials used in our study were obtained from the Materials Project (MP) database[30], and the compositional phase diagrams were constructed using the *pymatgen* package[31]. The mutual

reaction energy of the pseudo-binary was calculated using the same approach as defined in our previous work[26].

Electrochemical characterization. To measure the ionic conductivity of the garnet solid-state electrolyte, an Au paste was coated on both sides of the dense ceramic disk and acted as a blocking electrode. The gold electrodes were sintered at 700°C to form good contact with the ceramic pellet. Conductivities were calculated using $\sigma = L/(Z \times A)$, where Z is the impedance for the real axis in the Nyquist plot, L is the garnet ceramic disk length, and A is the surface area. The activation energies were obtained from the conductivities as a function of temperature using the Arrhenius equation. The hybrid solid-state cells were prepared in argon-filled glove box. 1M bis(trifluoromethane)sulfonimide lithium salt (LiTFSI, Sigma) in a mixture of dimethoxyethane (DME) and 1,3-dioxolane (DOL) (1:1 by volume) was used as the electrolyte for the hybrid solid-state Li-S batteries. Galvanostatic discharging and charging was measured using a cut-off voltage window of 1-3.5 V. The cell was then assembled into a 2032 coin cell with a highly conductive carbon sponge. The carbon sponge acted as the force absorber and prevented the garnet ceramic disk from being damaged. Battery test clips were used to hold and provide good contact with the coin cell. The edge of the cell was sealed with epoxy resin.

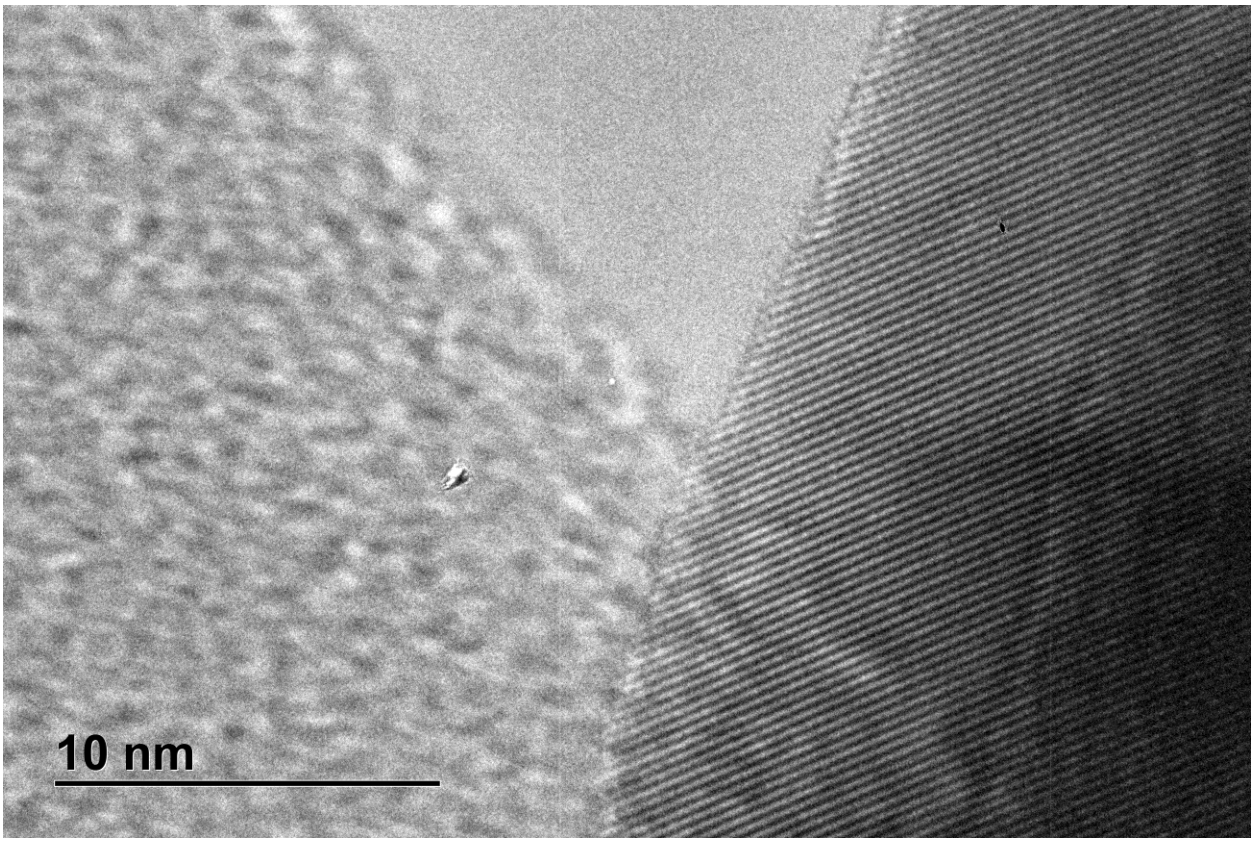

Figure S1. TEM of pristine garnet, showing highly crystalized grain and no amorphous region on surface.

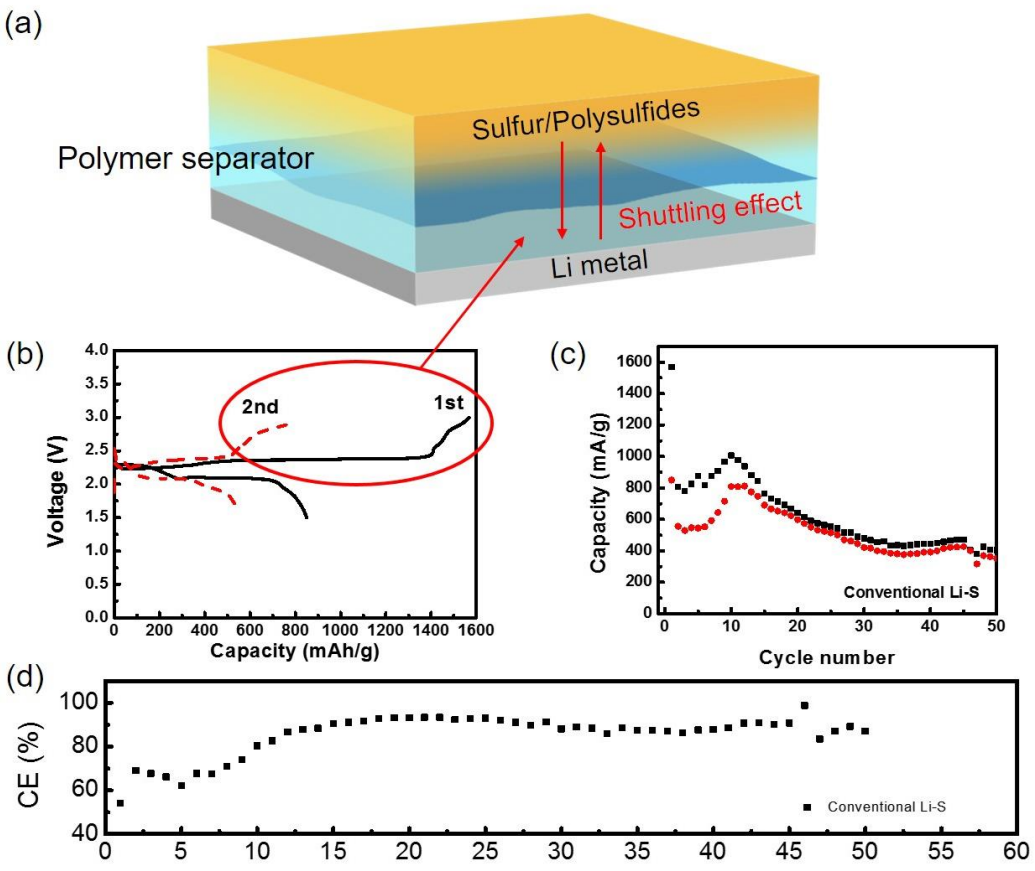

Figure S2. Control experiment of conventional Li-S battery using polymer separator membrane. The sulfur mass loading is ~1.2 mg/cm^2. (a) Schematic of shuttling effect in conventional Li-S battery. (b) Voltage profiles of conventional Li-S battery with a long charge plateau, indicating the shuttling effect of polysulfides. (c) Cycling performance of the conventional Li-S cell. The cell shows a fast decay after 10 cycles. (d) Coulombic efficiency of the conventional Li-S cell.

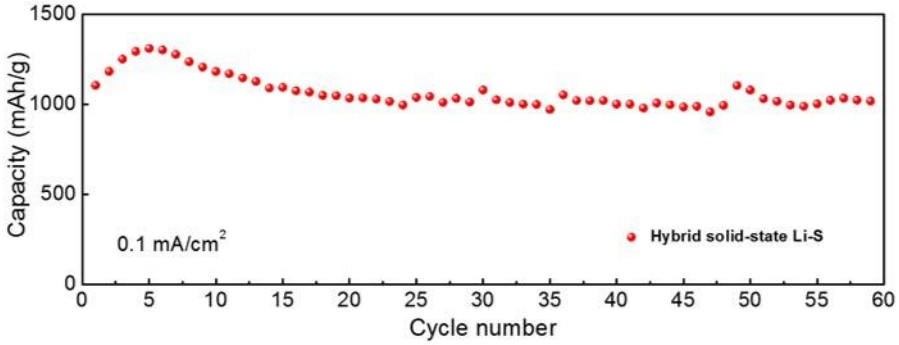

Figure S3. Cycling performance of hybrid garnet solid-state Li-S battery at a current of 0.1 mA/cm^2. The sulfur loading is 1.2 mg/cm^2. The hybrid cell delivered high capacity >1000 mAh/g with negligible capacity fade over 60 cycles, demonstrating no polysulfide shuttling.

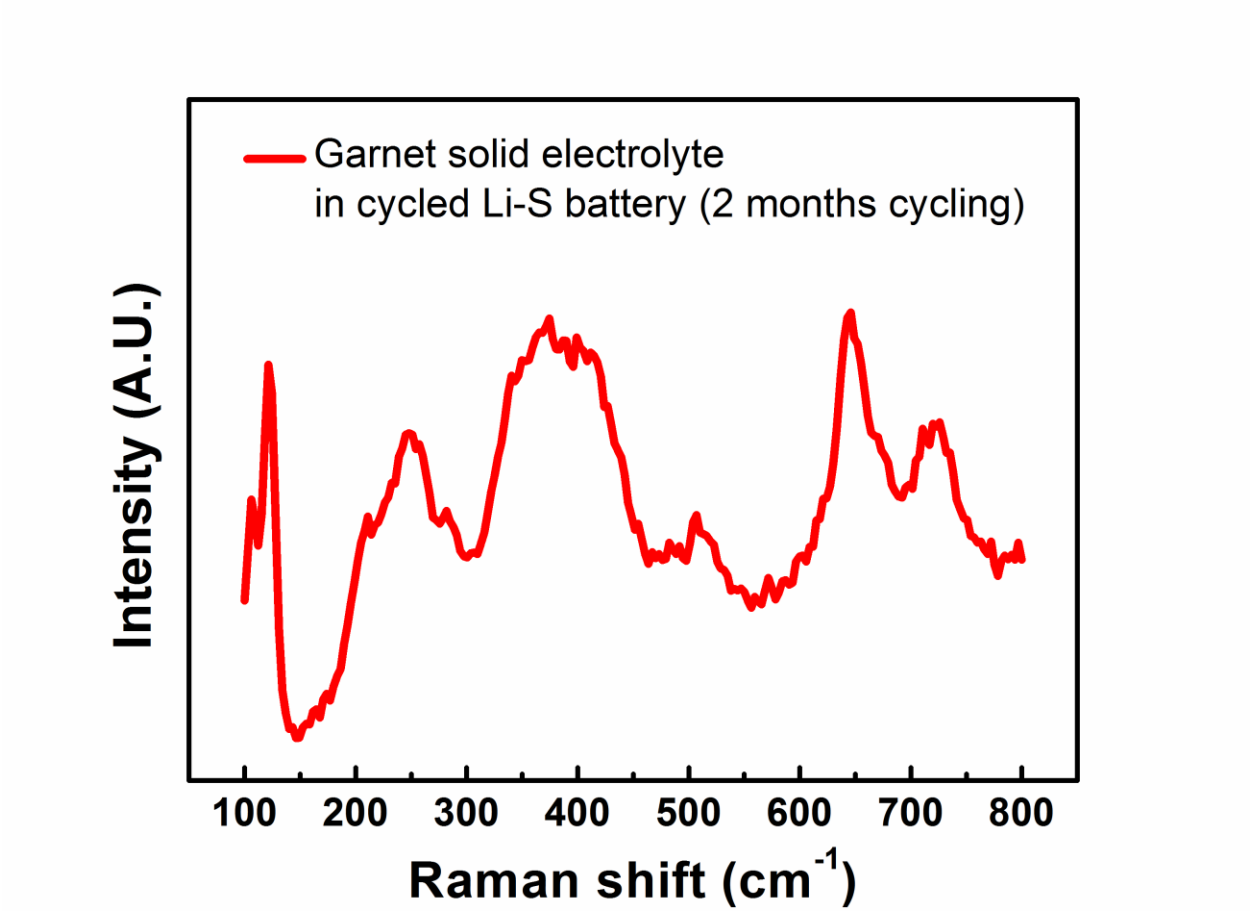

Figure S4. Raman spectrum of cycled garnet solid electrolyte in Li-S battery over 2 months cycling.

Table S1. The phase equilibria and decomposition energies of the Li-garnet $Li_7La_3Zr_2O_{12}$ and polysulfide Li_2S_8. Ratio *x* is the molar fraction of Li-garnet $Li_7La_3Zr_2O_{12}$ in the pseudo-binary composition (The parent composition of $Li_7La_3Zr_2O_{12}$ and polysulfide Li_2S_8 are already normalized to one atom per formula).

Ratio *x*	$\Delta E_{D,mutual}$ (meV/atom)	Phase Equilibria
0.520	-262.582	Li_2S, LaS_2, ZrS_3, Li_2SO_4
0.639	-246.345	Li_2S, ZrO_2, LaS_2, Li_2SO_4
0.721	-219.383	Li_2S, ZrO_2, LaSO, Li_2SO_4
0.771	-201.855	Li_2S, ZrO_2, La_2SO_2, Li_2SO_4
0.808	-181.707	Li_2S, Li_2SO_4, La_2SO_2, $La_2Zr_2O_7$
0.848	-156.986	Li_2S, La_2SO_2, Li_2ZrO_3, Li_2SO_4
0.894	-119.624	$Li_6Zr_2O_7$, Li_2SO_4, La_2SO_2, Li_2S
0.909	-103.100	$Li_6Zr_2O_7$, Li_2SO_4, La_2SO_2, Li_2O

ToC

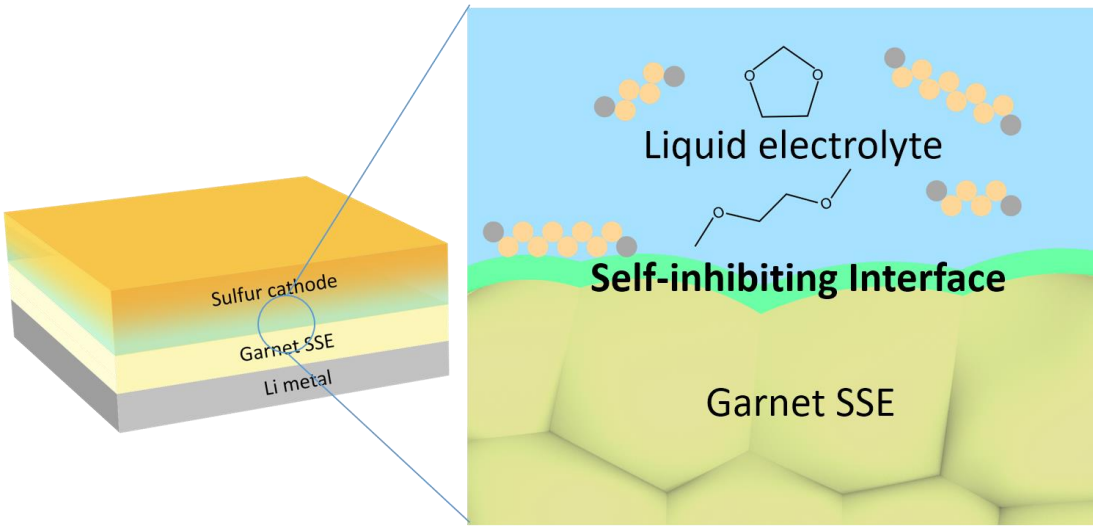
Sulfur cathode
Garnet SSE
Li metal
Liquid electrolyte
Self-inhibiting Interface
Garnet SSE